Adhesion of Nanosized Nickel Catalysts in the Nanocatalysis/UF System

Zhaoxiang Zhong, Weihong Xing, Wanqin Jin, and Nanping Xu
Membrane Science and Technology Research Center, Nanjing University of Technology, Nanjing 210009, P. R. China

DOI 10.1002/aic.11143
Published online March 29, 2007 in Wiley InterScience (www.interscience.wiley.com).

A system combining nanocatalytic reaction with crossflow ultrafiltration (UF) was used to prepare p-aminophenol from p-nitrophenol. In this system, nanosized nickel catalysts in suspension were employed during reaction, and then separated from slurry by an UF membrane filter. The adhesion of nickel particles to contact surfaces caused a rapid decline in the hydrogenation rate and UF flux. In order to understand the effect of materials properties, and operating parameters on adhesion of catalysts, the nickel adhesion was investigated by measuring the mass of nickel remaining on solid surfaces after contact. Surface materials with different roughness and hydrophilicity have been tested, such as poly(tetrafluoroethylene) (PTFE), stainless steel (AISI 304) and glass. The results show that rougher surfaces have more adhesion than smooth ones. Hydrophilic glass has less adhesion than hydrophobic PTFE, while intermediately hydrophilic stainless steel has the most adhesion due to its surface magnetic effect. During ultrafiltration, adhesion decreases with increasing crossflow velocity and increases with increasing suspension concentration. With the addition of microsized alumina particles in suspension, the adhesion of nanosized nickel can be inhibited effectively. © 2007 American Institute of Chemical Engineers *AIChE J,* 53: 1204–1210, 2007
Keywords: nanosized nickel, ultrafiltration, adhesion, surface properties, operating parameters

Introduction

In recent decades, nanocatalysts have found considerable applications in organic synthesis, environmental protection, photocatalysis, waste removal, fiber and mechanical industries.[1–2] Metal nanoparticles possess novel catalytic, optical and chemical properties, which have been correlated to their size and surface effect. It is reported that nanosized nickel shows better catalytic properties in the catalytic hydrogenation or dehydrogenation reaction.[3–6] However, the separation of ultrafine nickel particles from the reaction products creates another problem to be solved in practical applications.[7] A feasible approach to overcome this problem is to attach catalysts to a suitable substrate, but in that case, the effective surface area of the catalysts particles will be decreased. In fact, it is reported that catalysts in suspension have a better efficiency than immobilized ones.[8–10]

Du et al.[11] synthesized *p*-aminophenol from *p*-nitrophenol over nanosized nickel catalysts in laboratory. They mentioned the separation of catalysts from reaction products using a ceramic membrane, but they had no further description. In our research, a pilot-scale plant of nanocatalysis/UF system was set up to prepare *p*-aminophenol. Nanosized nickel was employed in its suspended form during reaction, and then separated from slurry by a ceramic membrane filter. We found that the hydrogenation rate decreased rapidly with recycling of catalysts in comparison with that in laboratory. The problem assumed to be due to adhesion of nickel particles to the surface of the pipeline, tanks and membrane during recovery of catalysts, which caused the decrease of catalysts concentration in reaction slurry, leading to a consequent decline in the reaction rate and permeate flux of the

Correspondence concerning this article should be addressed to N. Xu at npxu@njut.edu.cn.

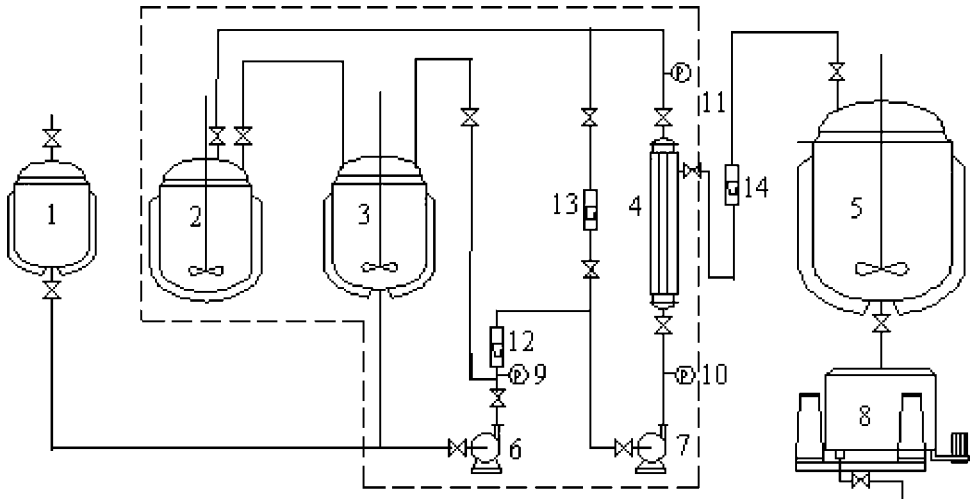

Figure 1. A pilot-scale nanocatalysis/UF system.

1. Solvent tank; 2. hydrogenation reactor; 3. intermediate tank; 4. membrane module; 5. crystallizer; 6. feed pump; 7. circulation pump; 8. centrifuge, 9.–11. pressure gauges, and 12.–14. rotameters.

membrane. Scarcely any reports address adhesion phenomena of catalysts in industry. This may be attributed to the following aspects: on the one hand, traditional industrial catalysts are usually with large particle size, and occurrence of adhesion is not easy due to perturbation of fluid flow; on the other hand, nanosized catalysts applied in industry are mostly still immobilized.

A particle in contact with a flat surface comprises two processes: first, the adhesion of particle on the surface that is kept by the physicochemical interactions; and second, the detachment of particle from the surface that is controlled by hydrodynamic interactions due to the flowing fluid.[12–13] In both processes, materials properties and operating parameters play an important role. In this research, we first investigated the effect of adhesion of nanosized nickel catalysts to contact surfaces on the nanocatalysis/UF system, and then attempt to find materials properties and operating parameters responsible for nickel adhesion. Our work was focused on: (1) desired surface materials that have low catalysts adhesion, and can be used as internal liner of pipeline, reactor and tanks, and (2) feasible methods that can inhibit the adhesion during ultrafiltration of nickel suspension. We try to make a contribution to develop a nanocatalysis/UF system to apply suspended nanosized catalysts in industrial production.

Experimental Section

Nanocatalysis/UF system

Figure 1 shows the pilot-scale plant, which consists of a hydrogenation reactor, a crossflow UF module and pumps, and so on. Hydrogenation reactor was a 100L continuous stirred-tank reactor. The configuration of the UF unit was tubular. It was fitted with one ZrO_2 membrane with a pore size of 50 nm (Jiusi, PR China), which has 19 channels with 4 mm inner dia. The effective membrane area was 0.24 m^2. The permeability of the new membrane was about 5,500 $L{\cdot}m^{-2}{\cdot}h^{-1}{\cdot}MPa^{-1}$, on the basis of pure water test at 25°C. The crossflow filtration was run at a temperature of 90 ± 2°C, crossflow velocity of 3m/s, and transmembrane pressure of 0.25MPa. The preparation of *p*-aminophenol was carried out in the same reaction conditions as that of the lab-scale experiment: temperature, 102°C; hydrogen partial pressure, 1.65 MPa; stirring rate, 300 rpm; initial nickel concentration 5 g/L.

The main experimental procedures are as follows: First, charging reactor with definite amounts of catalysts and *p*-nitrophenol in ethanol solution. During the hydrogenation reaction, catalysts were suspended in solution by violent stirring; Second, pressurizing the slurry into the intermediate tank after reaction, and adjusting the temperature and pressure, and Third, initiating feeder pump and circulation pump to start the membrane separation. The rejected catalysts were recycled to the reactor continuously and reused in the next batch of reaction, while the permeation entered the crystallizer. Finally, obtaining crystal *p*-aminophenol via centrifugal separation. Totally, one reaction cycle needed at least 3.5 h.

Adhesion Experiments about Materials Properties

Surface materials

The materials were chosen for their use in industrial equipments, and for their hydrophilic or hydrophobic properties. They were: PTFE (poly(tetrafluoroethylene)), stainless steel (AISI 304) and glass. Substrates of these materials were cut into conveniently sized substrates (8 cm × 2.5 cm × 0.1 cm), and cleaned prior to surface adhesion by washing in acetone and acid solution.

Roughness determination

Substrates employed were polished to different degrees using a rotating disc device and abrasive papers. The roughness was determined using an optical profilometer (AF-LI, HUST, PR China) used in vertical scanning interferometry mode (VSI) to map out the surface. The values of the rough-

ness were provided in terms of Ra (arithmetical mean deviation of the profile).[14]

Contact angle determination

Contact angles of liquids on solids were measured on the contact angle goniometer (JC2000A, Powereach, PR China), with a precision video camera coupled to image analysis. Water contact angle (θ_W) of three substrates increases in the order glass (20°) < stainless steel (58°) < PTFE (105°), as reported in literature.[15] Ethanol (95%) contact angle (θ_E) of PTFE is 35°, glass and stainless steel are entirely wetting.

Nanosized nickel catalysts

Nickel particles with diameter of 60 nm were applied in experiments. They were prepared by a chemical reduction method in a continuous reactor.[11]

Adhesion test

Adhesion test was carried out in the device as shown in Figure 2. Several substrates were immersed in the suspension of nanosized nickel with concentration of 5g/L. The suspension was stirred to prevent precipitation, and the temperature was kept at about 25°C by means of thermostatic water bath. Nickel adhering on the substrate was dissolved by nitric acid and measured with ICP (Optima2000 DV, PerkinElmer, USA). Adhesion amount was defined as follows

$$M_{ad} = \text{deposit weight/surface area } (\text{g} \cdot \text{m}^{-2}) \qquad (1)$$

This method is not aimed to measure the force acting between the first layer of particles and the solid surface, but to measure the global amount resulting from adhesion. This global adhesion corresponds to catalysts remaining on internal surface of equipments (for example, pipeline), and failing to recycle back to the reactor.

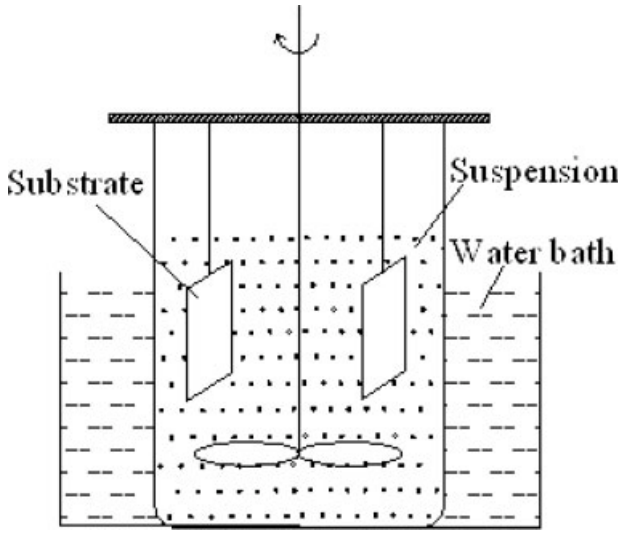

Figure 2. Device for measuring amount of nickel adhered.

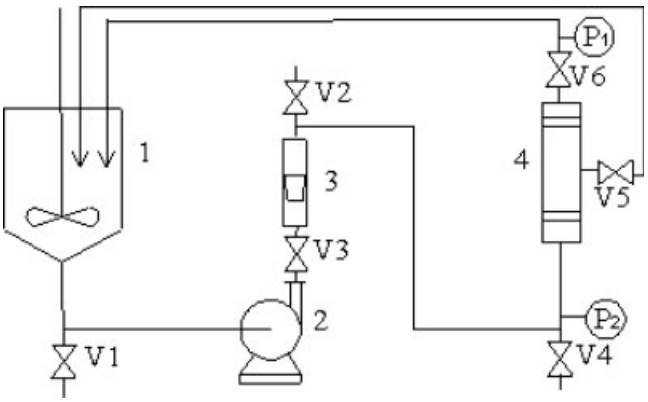

Figure 3. UF equipment.

1. Feed tank; 2. centrifugal pump; 3. rotameter; 4. membrane module; P1–P2. pressure gauges, and V1–V6. valves.

Adhesion experiments about operating parameters

We used UF equipment shown in Figure 3 to cycle the suspension of nanosized nickel in water, so as to investigate the effect of operating parameters on adhesion. The feed suspension was maintained at constant volume by recycling the permeation back into the feed tank. The effective membrane area was 0.12m^2. The capacity of the UF equipment was 0.165 $\text{m}^3 \cdot \text{h}^{-1}$ initially. The crossflow filtration was run at a temperature of 25 ± 1°C, operating pressure of 0.25 MPa, and crossflow velocity of 3–5 m/s. Concentration of suspension was measured by adding nitric acid into samples to dissolve nickel, and then analyzing with ICP. For the area of the material surface which suspension contact during filtration is difficult to determine, nickel adhesion during separation can be conveniently weighted by

$$M_{sep} = C_0 - C_t \qquad (2)$$

Where C_0 is initial concentration, and C_t is concentration of time t.

Results and Discussion

Effect of adhesion on the nanocatalysis/UF system

The correlations between the relative decline degree of hydrogenation rate, and the number of reaction cycles are shown in Figure 4. Throughout 13 continuous reaction cycles, the hydrogenation rate in lab-scale suffers 54% decline, while in pilot-scale it suffers 48% decline only throughout four continuous cycles. Maybe this is attributed to the scaleup effect, which always makes a remarkable difference between lab tests and pilot-scale.[16] On the other hand, it may be caused by mass loss of catalysts during membrane separation. Amount of catalyst recovered in reactor after every cycle was measured as in Figure 5. Its profile is similar to that of hydrogenation rate decline in pilot plant. Therefore, we concluded that mass loss of catalysts is mainly responsible for the decline of hydrogenation rate.

Previous experiments proved that nanosized nickel could be completely rejected by membranes,[7] so the mass loss of catalysts must result from adhesion of nickel particles to the internal surface of equipments. As shown in Figure 1, catalysts attached on the surface of pipelines, tanks and mem-

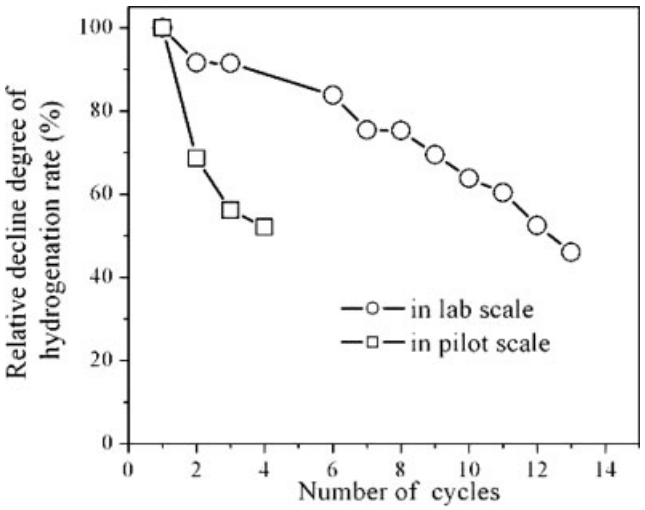

Figure 4. Variation of hydrogenation rate with reaction cycles.

Initial nickel concentration: 5 g/L.

branes in dash line scope, so that they cannot all recycle back to the hydrogenation reactor. As shown in Figure 5, the adhesion of catalysts to membrane surface also caused the fast decrease of average membrane flux in every UF operation.

Effect of Materials Properties on Adhesion

Surface roughness

Surface roughness plays an important role in adhesion. Large roughness results in large contact area between particles and surfaces,[17] and induces friction forces that resist particles rolling, and restrain their detachment from the surface.[18] On the other hand, rough surface can induce unsteady flows that are more effective than steady flows in re-entraining suspended particles near the surface.[19] As shown in Figure 6, amount of nickel adhered on stainless steel increased with the

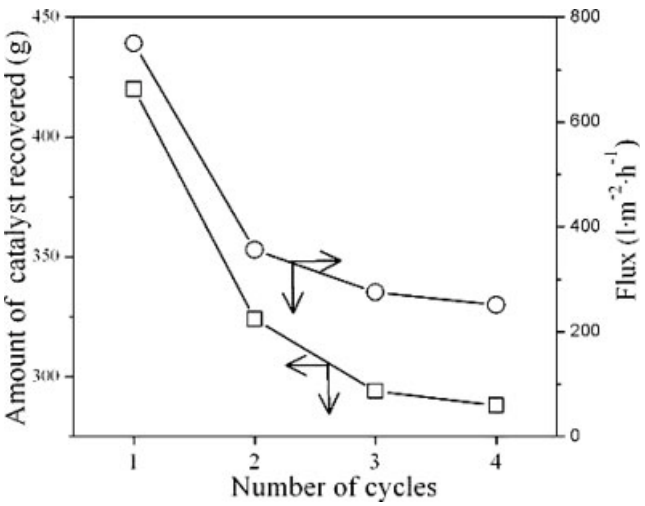

Figure 5. Variations of catalysts amount and permeate flux with cycles.

Initial nickel concentration: 5 g/L.

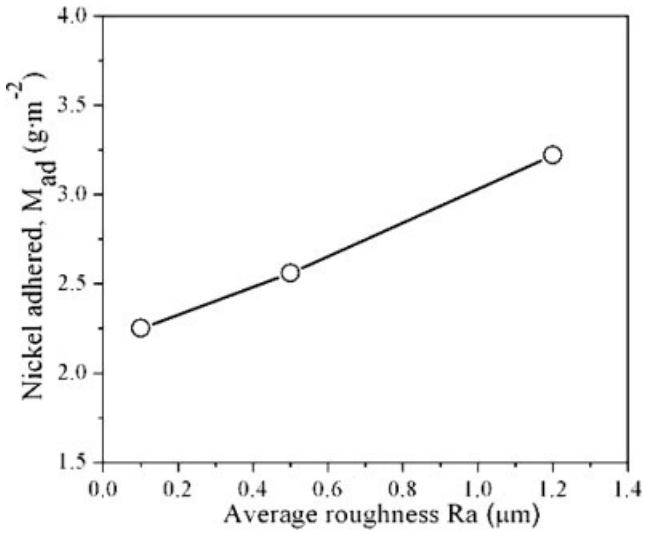

Figure 6. Effect of surface roughness on adhesion.

increase of average roughness. This was the combined result of the earlier two effects. The linear profiles of three substrates surfaces are taken with an optical profilometer along a direction orthogonal to the polishing direction, and are shown in Figure 7. Height variations and peak-to-peak distance appear much bigger for the rougher surface than for the smoother one. This enables more particles to position themselves in the valleys and makes their detachment difficult.

Surface hydrophilicity

Particle adhesion on solid surfaces from liquid suspensions involves *transport* and *attachment* steps: first particles transport from the bulk of a flowing suspension to the vicinity of solid surfaces, and second particles break the layer of water molecules adsorbed on the surface and contact directly the surface.[20–21] Adsorbed water layer is often called laminar boundary layer, which is thin and weak on hydrophobic surface, but thick and firm on hydrophilic surface for high-interfacial energy.[13] Therefore, hydrophilicity is one of the important surface properties governing the adhesion of particles to different substrates.

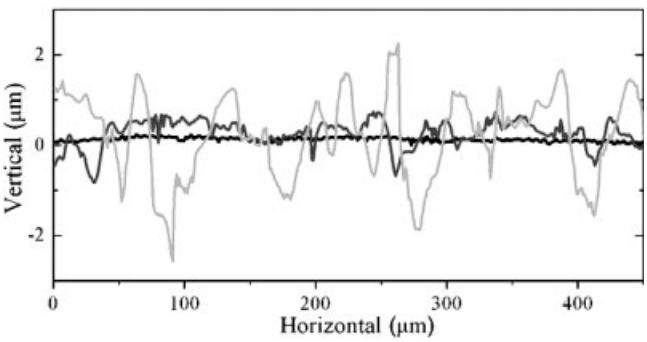

Figure 7. Typical 1-D profiles, orthogonal to the polish direction, of stainless steel surfaces taken with an optical profilometer (black, grey, light grey represent Ra = 0.1, 0.5, 1.2 μm, respectively).

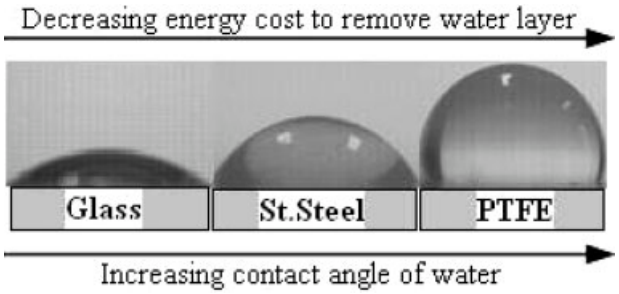

Figure 8. Effect of surface hydrophilicity on adhesion.

Effect of hydrophilicity of substrates on approach of particles is shown in Figure 8. Particles need less free energy to push away the water layer from the hydrophobic surface, thus, they can easily approach the separation distance that van der Walls force operates. Van der Walls force is a short-range interaction, and requires intimate contact between the particle and surface. The van der Waals interaction is taken to be $-AR/6h^2$, where R is the particle radius, h the minimum approach distance, and A the Hamaker constant $\approx 10^{-19}$ J.[13] As shown in this formula, van der Waals force is inversely proportional to the square of h, so the value of F_{ad} will depend on how far particles can penetrate into the adsorbed layer. Based on these analyses, the adhesion prediction should be in the order glass $<$ stainless steel $<$ PTFE. However, Figure 9a demonstrated that in water suspensions, adhesion amount of nickel on substrates increased in the order glass $<$ PTFE $<$ stainless steel. It had some discrepancy between the theoretical prediction and experimental result. Therefore, in addition to Van der Walls force, there must exit another interaction to enhance the adhesion of nickel on stainless steel.

Austenitic stainless steels are susceptible to martensitic transformation by plastic deformation. Metastable steels (for example, 301, 302, 304, 304L, 316 and 316L) may form martensites ε (hcp, paramagnetic) and α' (bcc, ferromagnetic), while stable steels (for example, 310) may only form martensite ε induced by plastic deformation.[22–23] 304 stainless steel is initially nonmagnetic, but its martensitic transformation during cold machining makes it magnetic or weakly magnetic. Moreover, larger deformation extent will result in more martensitic transformation, and, accordingly, increases the magnetization of stainless steel. The presence of martensite α' formed in an austenitic stainless steel can be measured by X-ray diffraction. Figure 10 showed the X-ray diffractogram of the stainless steel substrate in this study. Besides two peaks of austenite phase (γ), a peak of martensite phase (α') is observed, which came from machining (that is, cutting and polishing) deformation of the substrate. Meanwhile, nanosized nickel is known to be one of the most important magnetic materials,[24–25] so there exists an additional magnetic interaction between 304 stainless steel and nickel particle, which enhanced the attachment of nickel particles on stainless steel.

Compared with Figure 9a, and b showed the same adhesion order, but less adhesion amount on three substrates. This was attributed to higher interaction strength between ethanol and solid surfaces (contact angles of ethanol on substrates are much smaller than that of water) and ethanol formed stronger adsorbed layer than water, which was more difficult for particle to break. When in reaction slurry, Figure 9c indicated that addition of *p*-nitrophenol reduced the nickel adhesion. For the high surface area and surface chemical nature of nanosized nickel,[11] *p*-nitrophenol can be adsorbed onto the surface of nickel and form adsorbed layers. In most cases, these adsorbed layers caused the decrease of van der Walls force. The first reason was that adsorbed layers increased the distance between nickel particles and substrate surfaces; the second reason was that adsorbed layers had a negative effect on the Hamaker constant.[13,26–28]

The austenitic stainless steel can be demagnetized by a solution heat treatment, which makes a reverse transformation of martensite phase (α') to austenite phase (γ).[22,29–30] The stainless steel substrate was heated at a rate of $0.3^{\circ}C \cdot s^{-1}$ from room temperature in an inert atmosphere furnace, then kept at the temperature of 1050°C for 1 min, and rapidly water cooled to the ambient temperature.[30] The solution heat treatment had no effect on the surface roughness and hydrophilicity of the stainless steel. Its X-ray diffractogram showed that peak of martensite phase (α') disappeared, so

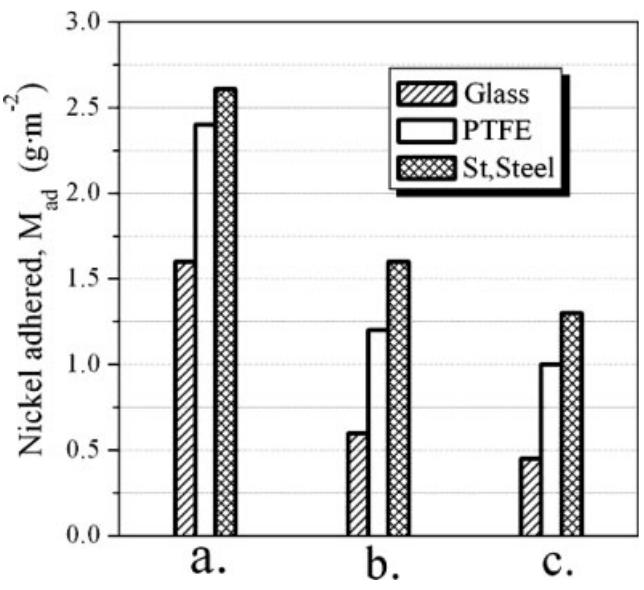

Figure 9. Adhesion of nanosized nickel in different suspensions.

a. In water, b. in ethanol, c. in solution of *p*-nitrophenol in ethanol.

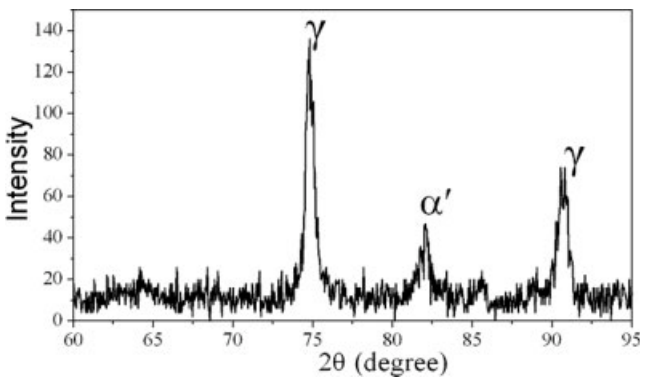

Figure 10. XRD pattern of stainless steel.

the substrate was nonmagnetic. Compared with magnetic stainless steel shown in Figure 9, nickel adhered on nonmagnetic stainless steel decreased to 2.10 g · m^2 in water, 0.93 g · m^2 in ethanol, and 0.74 g · m^2 in reaction slurry, respectively. So after demagnetization of stainless steel, the adhesion amount increased in the order of glass < stainless steel < PTFE.

From the discussion earlier, we can draw the conclusion that industrial equipment (for example, pipeline and reactor), should be internally lined with glass so as to reduce nickel adhesion, and metastable steel (for example, 304) equipment are not applicable in the treatment of nickel suspension for their surface magnetic effect. Furthermore, the surface of glass liner is always smooth enough to reduce nickel adhesion.

Effect of Operating Parameters on Adhesion

Crossflow velocity

During UF membrane separation, the effect of crossflow velocity on the nickel adhesion is shown in Figure 11. The initial concentration of suspension is 1g/L. The adhesion of nanosized nickel on internal surface of UF equipment (Figure 3), including feed tank, pipeline, membrane, and so on, decreased with increasing crossflow velocity. This was because deposition of particles was disturbed by the turbulence caused by flow at higher crossflow velocity. The shape of the curve in Figure 11 indicated that adhesion amount first increased sharply and then slowly. This was because at the beginning, attachment rate is much larger than detachment rate, and then the difference between two transport mechanisms decreases slowly.

Particle concentration of the suspension

The effect of suspension concentration on nickel adhesion and steady-state permeate flux of membrane was studied using six different concentrations: 1, 2.5, 5, 7.5, 10 and 12.5 g/L. The results are shown in Figure 12. Nickel adhesion first increased quickly and then slowly with increasing concentration, and approached a quasi-equilibrium state. Even though larger concentration enhanced the transport of particles to the solid surfaces, but which was limited by hydrodynamics and balanced by back-transport of particles from surfaces. After contact surfaces have reached their quasi-equilibrium state, they will adsorb little amount of nickel catalysts. The adhesion of fine particles to the membrane surface increased the cake resistance,[31] consequently, steady-state permeate flux declined in the trend opposite to the adhesion profile.

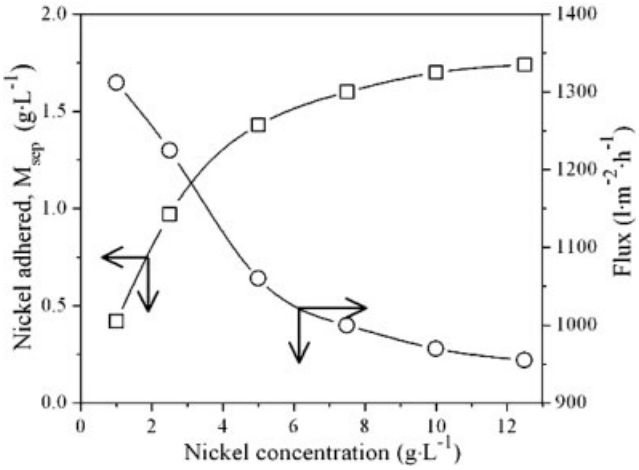

Figure 12. Effect of nickel concentration on adhesion and membrane flux.

Addition of microsized particles

Brownian forces and hydrodynamic forces are thought to be major detachment forces.[12,31–34] Microsized particles in suspension can provide another detachment mechanism. They enhance the nanosized nickel back-transport by scouring and thinning the adhesion layer. We investigated the effect of the weight ratio of α−alumina (α−Al_2O_3, average particle size 21 μm) to nanosized nickel on adhesion, and the result was shown as Figure 13. When the ratio increased

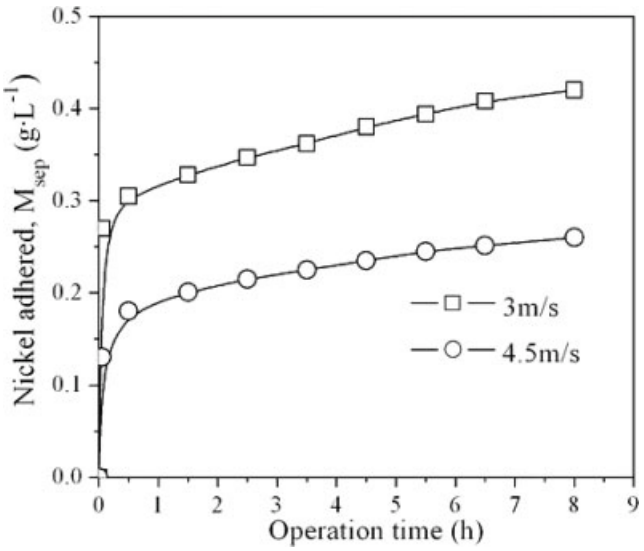

Figure 11. Effect of crossflow velocity on adhesion.

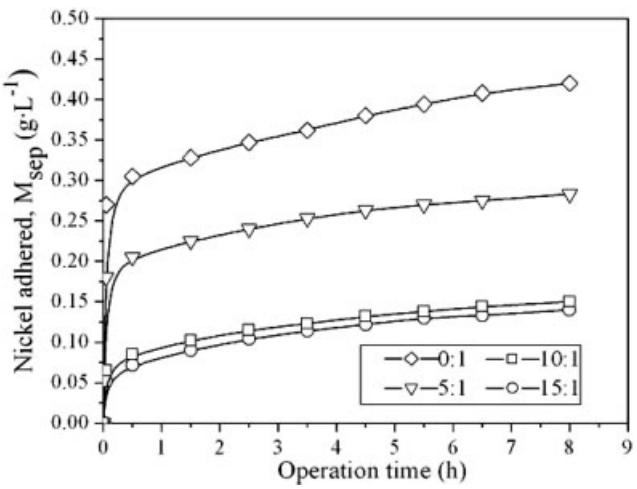

Figure 13. Effect of the weight ratio of Al_2O_3/Ni on adhesion.

Initial nickel concentration: 1 g/L.

to 10:1, adhesion of nanosized nickel decreased to the minimum. The result indicated that microsized particles could inhibit nanosized particles adhesion, but could not avoid the adhesion thoroughly. This was due to some nickel particles adhering to the pore of membrane and depositing in the valleys of rough surfaces (as shown in Figure 7). In addition, our previous research proved that adding inert particles in this reaction system has no evident effect on hydrogenation rate.[35]

Conclusion

In the nanocatalysis/UF system, nanosized nickel catalysts adhere to the internal surface of equipment, which leads to the decline of hydrogenation rate and permeate flux of membrane. Our research suggests that rougher surfaces have more adhesion, so the surface of the pipeline should be machined as smooth as possible. Glass has the least adhesion in nickel suspensions, while stainless steel has the most adhesion due to its surface magnetic effect. Therefore, it is applicable to make a glass liner on the internal surface of stainless steel pipeline and reactor when we apply nickel or other magnetic catalysts. The adhesion can be inhibited by increasing crossflow velocity, and adding microsized particles in nanosized nickel suspensions. Moreover, we can circulate nickel suspension in the system to make contact surfaces reach their adhesion quasi-equilibrium state previously, so that they will adsorb little nickel when the system runs.

Acknowledgments

This work is supported by the National Basic Research Program of China (No. 2003CB615702), the National Natural Science Foundation of China (No. 20436030), the Natural Science Foundation of Jiangsu (No. BK2006722), and Key Laboratory of Materials-Oriented Chemical Engineering of ministry of education.

Literature Cited

1. Gai PL, Roper R, White MG. Recent advances in nanocatalysis research. *Curr Opin Solid State Mater Sci*. 2002;6:401–406.
2. Yan Z. *Nanocatalysis Technology*. Beijing: Chemical Industry Press; 2003.
3. Gao J, Guan F, Zhao Y, Yang W, Ma Y, Lu X, Hou J, Kang J. Preparation of ultrafine nickel powder and its catalytic dehydrogenation activity. *Mater Chem Phys*. 2001;71:215–219.
4. Kapoor S, Salunke HG, Tripathi AK, Kulshreshtha SK, Mittal JP. Radiolytic preparation and catalytic properties of nanophase nickel metal particles. *Mater Res Bull*. 2000;35:143–148.
5. Wang H, Yu Z, Chen H, Yang J, Deng J. High activity ultrafine Ni-Co-B amorphous alloy powder for the hydrogenation of benzene. *Appl Catal A: Gen*. 1995;129:143–149.
6. Zuo D, Zhang Z, Cui Z. Catalytic properties of nanometer nickel ultrafine particles in nitrobenzene hydrogenation. *Chin J Mol Catal*. 1995;9:298–302.
7. Chen R. *Study and Application of Coupling Nanocatalysis and Ingorganic Membranes*. Nanjing University of Technology: Nanjing, China; 2004. Ph.D. thesis.
8. Lee S, Choo K, Lee C, Lee H, Hyeon T, Choi W, Kwon H. Use of Ultrafiltration membranes for the separation of tio_2 photocatalysts in drinking water treatment. *Ind Eng Chem Res*. 2001;40:1712–1719.
9. Li X, Zhao Y. Advanced treatment of dyeing wastewater for reuse. *Water Sci Technol*. 1999;39:249–255.
10. Nagahara H, Mitsuo K. *Process for producing cycloolefins*. US 4734536; 1988.
11. Du Y, Chen H, Chen R, Xu N. Synthesis of p-aminophenol from p-nitrophenol over nanosized nickel catalysts. *Appl Catal A: Gen*. 2004;277:259–264.
12. Yiantsios SG, Karabelas AJ. Detachment of spherical microparticles adhering on flat surfaces by hydrodynamic forces. *J Colloid Interface Sci*. 1995;176:74–85.
13. Israelachvili J. *Intermolecular and Surface Forces*. 2nd ed. New York: Academic Press; 1992.
14. Chiche A. Pareige P. Creton C. Role of surface roughness in controlling the adhesion of a soft adhesive on a hard surface. *C R Acad Sci Ser IV: Phys*. 2000;1:1197–1204.
15. Michalski MC, Desobry S, Babak V, Hardy J. Adhesion of food emulsions to packaging and equipment surfaces. *Colloids Surf A*. 1999;149:107–121.
16. Bisio A, Kabel R. *Scaleup of chemical processes-Conversion from Laboratory scale tests to successful commercial size design*. New York: John Wiley & Sons; 1985.
17. Gallardo-Moreno AM, González-Martín ML, Bruque JM, Pérez-Giraldo C. The adhesion strength of Candida parapsilosis to glass and silicone as a function of hydrophobicity, roughness and cell morphology. *Colloids Surf A*. 2004;249:99–103.
18. Kostoglou M, Karabelas AJ. Effect of Roughness on Energy of Repulsion between Colloidal Surfaces. *J Colloid Interface Sci*. 1995;171:187–199.
19. Belfort G, Davis RH, Zydney AL. The behavior of suspensions and macromolecular solutions in crossflow microfiltration. *J Membr Sci*. 1994;96:1–58.
20. Yiantsios SG, Karabelas AJ. The effect of gravity on the deposition of micron-sized particles on smooth surfaces. *Int J Multiphase Flow*. 1998;24:283–293.
21. Vakarelski IU, Ishimura K, Higashitani K. Adhesion between silica particle and mica surfaces in water and electrolyte solutions. *J Colloid Interface Sci*. 2000;227:111–118.
22. Tavares SSM, Fruchart D, Miraglia S. A magnetic study of the reversion of martensite α' in a 304 stainless steel. *J Alloys Compd*. 2000;307:311–317.
23. Ding J, Huang H, McCormick PG, Street R. Magnetic properties of martensite-austenite mixtures in mechanically milled 304 stainless steel. *J Magn Magn Mater*. 1995;139:109–114.
24. Zhang HT, Wu G, Chen XH, Qiu XG. Synthesis and magnetic properties of nickel nanocrystals. *Mater Res Bull*. 2006;41:495–501.
25. Hou YL, Gao S. Solvothermal reduction synthesis and magnetic properties of polymer protected iron and nickel nanocrystals. *J Alloys Compd*. 2004;365:112–116.
26. Mahanty J, Ninham BW. *Dispersion Forces*. London: Academic Press; 1976.
27. Sato T, Ruch R. *Stabilization of colloidal dispersion by polymer adsorption*. New York: Marcel Dekker; 1980.
28. Lu S. *Industrial Suspensions-Properties, Preparation and Processing*. Beijing: China: Chemical Industry Press; 2003.
29. Feng Z, Song L. Magnetism elimination of the cold-formed stainless steel head. *Petrochem Equip. (in Chinese)*. 2002;31:47–48.
30. Fujita T. *The heat treatment of stainless steel*. Tokyo: Diumal Industry News Service; 1970.
31. Ripperger S, Altmann J. Particle deposition and layer formation at the crossflow microfiltration. *J Membr Sci*. 1997;124:119–128
32. Fane AG, Ultrafiltration of suspensions. *J Membr Sci*. 1984;20:249–259.
33. Kolakowski JE, Matijevic E. Particle adhesion and removal in model systems. Part 1. Monodispersed chromium hydroxide on glass. *J Chem Soc Faraday Trans*. 1979;75:65–78.
34. Kuo RJ, Matijevic E. Particle adhesion and removal in model systems. Part 2. Monodispersed chromium hydroxide on steel. *J Chem Soc Faraday Trans*. 1979;75:2014–2026.
35. Zhong Z, Chen R, Xing W, Xu N, Recovery of nanometer nickel catalyst with ceramic membrane. *Chin J Chem Ind Eng. (in Chinese)*. 2006;57:849–852.

Manuscript received Oct. 8, 2006, and revision received Feb. 3, 2007.